Available online at www.sciencedirect.com
ScienceDirect
Journal of Power Sources 164 (2007) 73–79
JOURNAL OF POWER SOURCES
www.elsevier.com/locate/jpowsour

Short communication

Thermodynamic analysis of carbon formation boundary and reforming performance for steam reforming of dimethyl ether

Kajornsak Faungnawakij [a,b], Ryuji Kikuchi [b,*], Koichi Eguchi [b]

[a] *Japan Science and Technology Agency (JST), Innovation Plaza Kyoto, 1-30 Goryo-Ohara Nishikyo-ku, Kyoto 615-8245, Japan*
[b] *Department of Energy and Hydrocarbon Chemistry, Graduate School of Engineering, Kyoto University, Nishikyo-ku, Kyoto 615-8510, Japan*

Received 14 September 2006; received in revised form 26 September 2006; accepted 27 September 2006
Available online 9 November 2006

Abstract

Thermodynamic analysis of dimethyl ether steam reforming (DME SR) was investigated for carbon formation boundary, DME conversion, and hydrogen yield for fuel cell application. The equilibrium calculation employing Gibbs free minimization was performed to figure out the required steam-to-carbon ratio (S/C = 0–5) and reforming temperature (25–1000 °C) where coke formation was thermodynamically unfavorable. S/C, reforming temperature and product species strongly contributed to the coke formation and product composition. When chemical species DME, methanol, CO_2, CO, H_2, H_2O and coke were considered, complete conversion of DME and hydrogen yield above 78% without coke formation were achieved at the normal operating temperatures of molten carbonate fuel cell (600 °C) and solid oxide fuel cell (900 °C), when S/C was at or above 2.5. When CH_4 was favorable, production of coke and that of hydrogen were significantly suppressed.

Keywords: Thermodynamic analysis; Carbon formation boundary; Dimethyl ether; Steam reforming; Fuel cell; Hydrogen

1. Introduction

Fuel cells are presented as an efficient power generator applicable to both mobile and stationary use. In typical, an electrochemical reaction of a fuel at anode (generally hydrogen) and an oxidant at cathode (generally oxygen) generates electricity through a fuel cell. Several types of fuel cell have been developed, for example, polymer electrolyte fuel cell (PEFC), solid oxide fuel cell (SOFC), and molten carbonate fuel cell (MCFC). PEFC provides high power density and operates at low temperature of ca. 80 °C. These features make it suitable for vehicle application. However, carbon monoxide in the fuel feed is limited generally below 10 ppm since it poisons Pt anode of the fuel cell, especially at such low temperature. Therefore, pure hydrogen or external fuel reformer with CO remover is needed for PEFC. Unlike PEFC, SOFC and MCFC operate at high temperatures of 700–1000 and 600–650 °C, respectively. Both external and internal fuel reformers are applicable to these types of fuel cells. In the case of the internal reforming, hydrogen is produced by the reforming reaction taking place on the fuel cell anode or inside the fuel cell chamber. In addition, intermediate temperature fuel cells operating at 400–600 °C has been presently developed.

Various types of hydrogen production systems have been extensively studied. Hydrogen is an environmentally friendly fuel since it does not release carbon dioxide on site when employed in fuel cell processor. Several hydrogen-generating techniques, i.e. steam reforming, partial oxidation, and autothermal reforming of various fuels, e.g. gasoline, LPG, methane, methanol (MeOH), ethanol (EtOH), and dimethyl ether (DME), have been regarded as the efficient processes for deployment of fuel cell systems. Presently, DME is recognized as a promising alternative hydrogen source. Of DME synthesis, MeOH is first synthesized from syngas over metal catalysts for example Cu-based catalysts [1–4]. Subsequently, dehydration of MeOH to DME takes place over solid-acid catalysts for example zeolite and alumina [1–4]. Several large DME plants are currently under construction [5]. The large scale production will decrease the cost of DME even though the cost of DME is still controversial. DME and MeOH are suitable for on-board reforming because they can easily be liquefied and be reformed at low temperature

* Corresponding author. Tel.: +81 75 383 7059; fax: +81 75 383 2521.
E-mail addresses: kajornsak@kyoto.jst-plaza.jp, kajornsak_f@yahoo.com (K. Faungnawakij), rkikuchi@mbox.kudpc.kyoto-u.ac.jp (R. Kikuchi).

0378-7753/$ – see front matter © 2006 Elsevier B.V. All rights reserved.
doi:10.1016/j.jpowsour.2006.09.072

Nomenclature

a_{ik}	number of atoms of the kth element present in each molecule of species i
A_k	total mass of kth element in the feed
$\hat{f}_i$	the fugacity of species i in system
f_i^0	the standard-state fugacity of species i
F_{DMEin}	molar flow rate of DME at inlet
F_{DMEout}	molar flow rate of DME at outlet
$F_{\mathrm{H_2out}}$	molar flow rate of hydrogen at outlet
$G_{\mathrm{C(S)}}$	molar Gibbs free energy of solid carbon
$\bar{G}_{\mathrm{C(g)}}$	partial molar Gibbs free energy of gas carbon
$\bar{G}_{\mathrm{C(S)}}$	partial molar Gibbs free energy of solid carbon
$\Delta G^\circ_{f_{\mathrm{C(S)}}}$	standard Gibbs function of formation of solid carbon
$\Delta G^\circ_{f_i}$	standard Gibbs function of formation of species i
G_i°	standard Gibbs free energy of species i
$\bar{G}_i$	partial molar Gibbs free energy of species i
G^{t}	total Gibbs free energy
n_{c}	mole of carbon
N	number of species in the reaction system
P	pressure of system (kPa)
P^0	standard-state pressure of 101.3 kPa
R	molar gas constant
T	temperature of system (°C)
T_{c}	temperature at which the first disappearance of carbon was achieved (°C)
T_{r}	reforming temperature (°C)
y_i	gas phase mole fraction

Greek symbols

$\widehat{\phi}_i$	fugacity coefficient of species i
λ_k	Lagrange multiplier
μ_i	chemical potential of species i

of 200–350 °C for MeOH and 200–450 °C for DME. DME is less toxic and therefore is preferable to MeOH. Reforming of DME is expected to match with wide range operating temperature of fuel cells. Development of catalysts for DME reforming has been currently carried out [6–12]. Durability of the DME reforming catalyst is one of the key factors for the practical use. Carbon (coke) formation and metal sintering are known as main reasons for deactivation. Operating the reforming at appropriate condition can suppress such deactivation. Several reports calculated the thermodynamic composition of reforming processes such as MeOH SR [13], methane dry reforming [14], and EtOH SR [15] to figure out the condition to avoid the formation of coke. Thermodynamic composition of DME SR was recently reported [16]. Carbon formation was not however considered in the calculation.

In the present study, thermodynamic equilibrium of DME–steam reforming in an external reformer for fuel cell applications was studied. Influences of steam-to-carbon ratio (S/C = 0–5) and reforming temperature (25–1000 °C) on carbon formation boundary, DME conversion, and hydrogen yield were evaluated by using Gibbs free minimization technique.

2. Modeling and simulation methodology

2.1. Minimization of Gibbs free energy

Gibbs free energy is the most commonly used function to identify the equilibrium state. A minimization of total Gibbs free energy is an appropriate method to calculate the equilibrium compositions of any reacting system [17]. The total Gibbs free energy of a system is given by the sum of ith species:

$$G^{\mathrm{t}} = \sum_{i=1}^{N} n_i \bar{G}_i = \sum_{i=1}^{N} n_i \mu_i = \sum n_i G_i^\circ + R(T + 273.15) \sum n_i \ln \frac{\hat{f}_i}{f_i^0} \quad (1)$$

where G^{t} is the total Gibbs free energy, $\bar{G}_i$ the partial molar Gibbs free energy of species i, G_i° the standard Gibbs free energy, μ_i the chemical potential, R the molar gas constant, T the temperature of system, P the pressure of system, $\hat{f}_i$ the fugacity in system, f_i^0 the standard-state fugacity, and n_i is the mole of species i. For reaction equilibria in gas phase, $\hat{f}_i = y_i \widehat{\phi}_i P$, $f_i^0 = P^0$, and $G_i^\circ = \Delta G^\circ_{f_i}$ are assumed. By using the Lagrange multiplier method, the minimum Gibbs free energy of each gaseous species and that of the total system can be expressed as Eqs. (2) and (3), respectively:

$$\Delta G^\circ_{f_i} + R(T + 273.15) \ln \frac{y_i \widehat{\phi}_i P}{P^0} + \sum_k \lambda_k a_{ik} = 0 \quad (2)$$

$$\sum_{i=1}^{N} n_i \left(\Delta G^\circ_{f_i} + R(T + 273.15) \ln \frac{y_i \widehat{\phi}_i P}{P^0} + \sum_k \lambda_k a_{ik} \right) = 0 \quad (3)$$

with the constraining equation:

$$\sum_i n_i a_{ik} = A_k$$

where $\Delta G^\circ_{f_i}$ is the standard Gibbs function of formation of species i, P^0 the standard-state pressure of 101.3 kPa, y_i the gas phase mole fraction, $\widehat{\phi}_i$ the fugacity coefficient of species i, λ_k the Lagrange multiplier, a_{ik} the number of atoms of the kth element present in each molecule of species i, and A_k is the total mass of kth element in the feed.

When solid carbon (graphite) is involved in the system, exploiting the vapor–solid phase equilibrium is applied to the Gibbs-energy of carbon as shown in Eq. (4). Substituting Eq. (1) by Eq. (2) for gaseous species and by Eq. (4) for solid species gives the minimization function of Gibbs-energy as following Eq. (5):

$$\bar{G}_{\mathrm{C(g)}} = \bar{G}_{\mathrm{C(S)}} = G_{\mathrm{C(S)}} \cong \Delta G^\circ_{f_{\mathrm{C(S)}}} = 0 \quad (4)$$

$$\sum_{i=1}^{N-1} n_i \left(\Delta G^{\circ}_{f_i} + R(T + 273.15) \ln \frac{y_i \widehat{\phi}_i P}{P^0} + \sum_k \lambda_k a_{ik} \right) + (n_c \Delta G^{\circ}_{f_{C(S)}}) = 0 \quad (5)$$

where $\bar{G}_{C(g)}$, $\bar{G}_{C(S)}$, $G_{C(S)}$, $\Delta G^{\circ}_{f_{C(S)}}$ and n_c are the partial molar Gibbs free energy of gas carbon, that of solid carbon, the molar Gibbs free energy of solid carbon, the standard Gibbs function of formation of solid carbon, and mole of carbon, respectively.

The equilibrium calculations employing the Gibbs-energy minimization were done with the Aspen plus, Aspen Tech™. The program is capable to simulate a single phase or multiphase of multicomponent in equilibria. The steam-to-carbon ratio S/C and the reforming temperature T_r were varied in the range of 0–5 and 25–1000 °C, respectively. The pressure was fixed at 1 atm in this study. The equation of state used in the calculation was the Peng Robinson method. To perform the calculation, reactant and product species with their proportion along with reaction conditions, i.e. temperature and pressure have to be clarified. Then the minimization could be performed to calculate the equilibrium composition.

2.2. DME SR in external reformer

The major gas species involved in the DME SR are CH_3OCH_3, CH_3OH, H_2O, H_2, CO, CO_2, CH_4 and coke, based on experimental observations [6–12]. The basis set of compounds is, therefore, acceptable for practical condition. Steam reforming of DME (Eq. (6)) is a two-step reaction, namely, hydrolysis of DME to MeOH (Eq. (7)), followed by steam reforming of MeOH (Eq. (8)). DME hydrolysis actively takes place over acidic sites of acid catalysts such as alumina and zeolite, while MeOH SR proceeds over metal catalysts, Cu-, Pd-, and Pt-based catalysts. Besides DME SR, reverse water gas shift reaction (r-WGSR as Eq. (9)) generally proceeds over such metal catalysts during the reforming process. In addition, methane can be generated via DME decomposition (Eq. (10)) in the case that strong acidic catalyst or high reforming temperature is employed and via CO methanation (Eq. (11)) in the case Ni-based catalysts or precious metal catalysts are used:

$$\text{DMESR}: \quad (CH_3)_2O + 3H_2O \leftrightarrow 6H_2 + 2CO_2 \quad (6)$$

$$\text{DMEhydrolysis}: \quad (CH_3)_2O + H_2O \leftrightarrow 2CH_3OH \quad (7)$$

$$\text{MeOHSR}: \quad CH_3OH + H_2O \leftrightarrow 3H_2 + CO_2 \quad (8)$$

$$\text{r-WGSR}: \quad O_2 + H_2 \leftrightarrow H_2O + CO \quad (9)$$

$$\text{DMEdecomposition}: \quad (CH_3)_2O \leftrightarrow CH_4 + CO + H_2 \quad (10)$$

$$\text{COmethanation}: \quad CO + 3H_2 \leftrightarrow CH_4 + H_2O \quad (11)$$

Carbon formation boundary was determined by adding carbon (graphite) as a solid form into the basis set. The temperature, at which the first disappearance of carbon T_c was achieved, was considered as a carbon boundary. The regions above and below the boundary are the coke-free and coke-formed regions, respectively. All plausible products DME, MeOH, H_2O, H_2, CO, CO_2, CH_4, and graphite were taken into account as *Case 1*. Methane formation can be suppressed by using copper catalyst or non-acidic catalyst and therefore methane was excluded from the calculation as *Case 2*. *Cases 3* and *4* were set for the case when carbon formation was not considered.

- *Case 1*. CH_3OCH_3, CH_3OH, H_2O, H_2, CO, CO_2, C (graphite), and CH_4.
- *Case 2*. CH_3OCH_3, CH_3OH, H_2O, H_2, CO, CO_2, and C (graphite).
- *Case 3*. CH_3OCH_3, CH_3OH, H_2O, H_2, CO, and CO_2.
- *Case 4*. CH_3OCH_3, CH_3OH, H_2O, H_2, CO, CO_2, and CH_4.

2.3. DME conversion and hydrogen yield

To evaluate the performance of the steam reforming system, the equilibrium conversions of DME and yield of H_2 are defined as follows:

$$\text{equilibrium conversion of DME}\,(\%) = \frac{F_{\text{DMEin}} - F_{\text{DMEout}}}{F_{\text{DMEin}}} \times 100 \quad (12)$$

$$H_2\ \text{yield}\,(\%) = \frac{F_{H_2\text{out}}}{F_{\text{DMEin}}} \times \left[\frac{\text{DME}}{H_2}\right]_T \times 100 \quad (13)$$

where F_{DMEin} and F_{DMEout} are the molar flow rates of DME at inlet and outlet, respectively, and $F_{H_2\text{out}}$ is molar flow rate of hydrogen at outlet. $[\text{DME}/H_2]_T = [1/6]$ is the theoretical mole ratio of DME fed and hydrogen produced (see Eq. (6)).

3. Results and discussion

3.1. Coke formation boundary

Formation of coke during the catalytic steam reforming could lead to deactivation of catalysts, resulting in low durability and activity. Thus it is important to keep it under control. Operating the reforming system under the coke-free region could avoid the coke formation. We have evaluated the temperature region where coke is present or absent in the reforming products. When coke with methane or coke is thermodynamically favored, the basis sets Case1 and Case2 were used for the calculation. Besides CO and CO_2, CH_4 was considered as the most abundant carbon-containing gaseous product produced during DME SR.

The most probable reactions leading to carbon formation are listed below:

$$2CO \leftrightarrow CO_2 + C \quad (14)$$

$$CH_4 \leftrightarrow 2H_2 + C \quad (15)$$

$$CO + H_2 \leftrightarrow H_2O + C \quad (16)$$

$$CO_2 + 2H_2 \leftrightarrow 2H_2O + C \quad (17)$$

$$(CH_3)_2O \leftrightarrow H_2O + 2H_2 + 2C \quad (18)$$

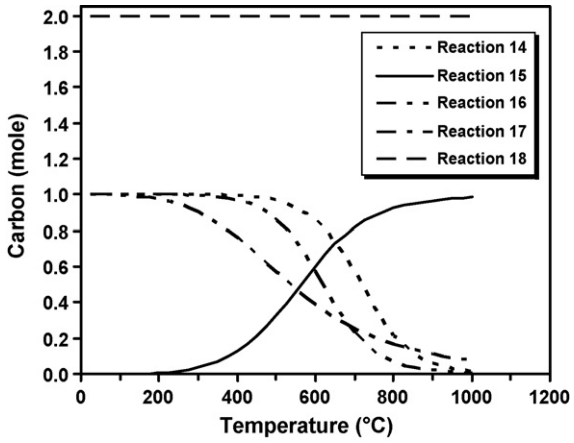

Fig. 1. Coke formation via reactions (14)–(18) as a function of temperature.

Fig. 1 shows the carbon formation as a function of temperature via each reaction. This is to determine the role of each reaction on carbon formation thermodynamically. Reactions (16) and (17) are thermodynamically unfavorable at low temperature than reaction (14) (Boudouard reaction), while reaction (15) is favorable at high temperature. Reaction (18) is favorable throughout the temperature range studied, since the system is not included other carbon-containing compounds, such as, CO, CO_2, and CH_4.

Fig. 2a and b illustrates the ratio of coke formed per DME fed in DME SR as a function of S/C and temperature. In Fig. 2a (Case 1), coke was always produced when S/C is less than 0.5. Approximately 1 mole of coke was formed by 1 mole of DME in the absence of steam. At a given temperature, increase in S/C lowered the coke formation. Increase in temperature resulted in decrease in coke production except in the temperature range of ca. 400–600 °C. However, further increase in temperature above 600 °C could inhibit coke formation. This is because steam reforming and CO_2 reforming of methane strongly contributed to the methane removal [18]. In Fig. 2b (Case 2), when CH_4 was exclude from the basis set, coke was always produced when S/C is less than 0.5. Two moles of coke was formed by 1 mole of DME in the temperature range below 200 °C, corresponding to the DME decomposition, reaction (18). Increase in temperature and S/C suppressed the coke formation by concomitant contribution of reverse reactions (14), (16), and (17).

Coke formation boundary was plotted as a function of S/C ratio as shown in Fig. 3. In Case 1, the T_c drastically decreased from ca. 1100 to 200 °C as S/C increased from 0.5 to 1.75. Further increase in S/C from 1.75 to 5 gradually decreased T_c from 200 to 25 °C. In Case 2 when methane was not taken into account, T_c decreased from ca. 900 to 500 °C, when the S/C ratio increased from 0.5 to 5. The temperature at which carbon was unfavorable coincided well with the operating temperature of MCFC and SOFC. When S/C is lower than 0.5, the coke was still present even at high temperature above 2000 °C for both cases. When DME SR is operated under the coke-formed region, the catalyst that has high resistance to coke formation should be used. Considering Case 2 when selectivity to CH_4 is zero, the catalyst with high thermal durability is required for reforming DME in the coke-free region at high temperatures.

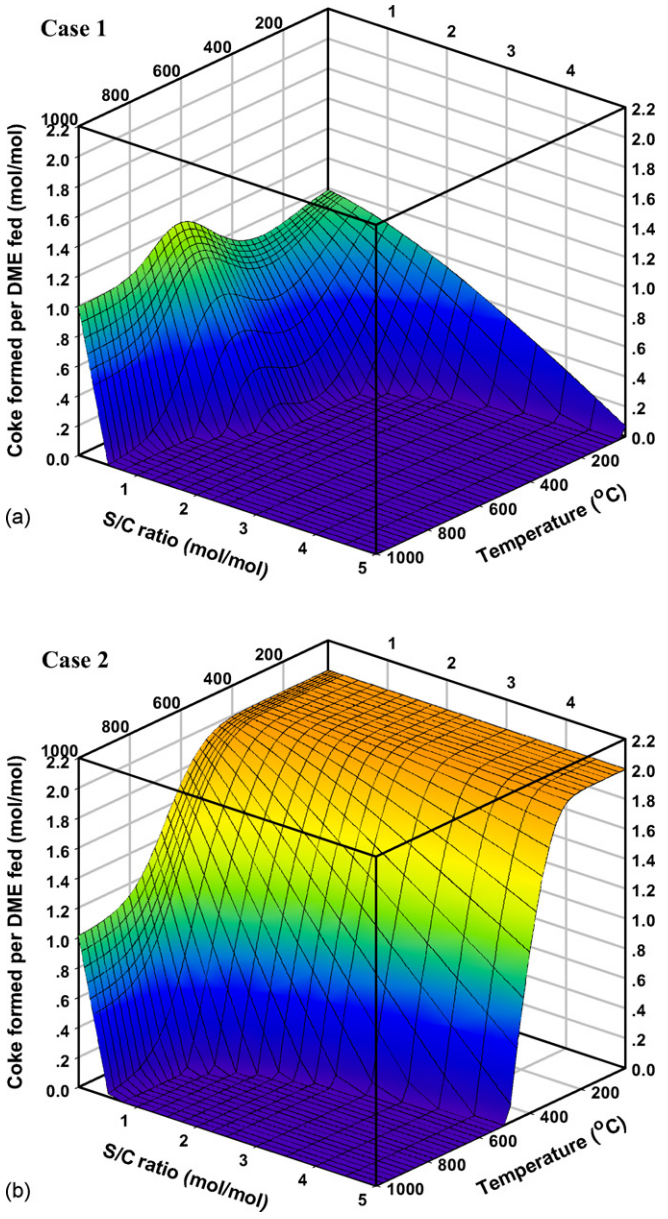

Fig. 2. Coke formation from DME SR as a function of steam-to-carbon (S/C) and temperature: (a) Case 1 and (b) Case 2.

3.2. DME conversion

Fig. 4 shows the conversion of DME as a function of S/C and temperature. In Fig. 4a, DME was completely converted throughout the operating condition studied in the presence of coke and/or methane (Cases 1, 2, and 4). Thermodynamically DME can be converted to methane and coke even at low temperatures. In Case 2, DME was decomposed via reaction (18). When methane is favorable, it could be formed instead of coke and hydrogen at the low temperature zone. In Fig. 4b (Case 3), when coke and methane are not taken into account, complete

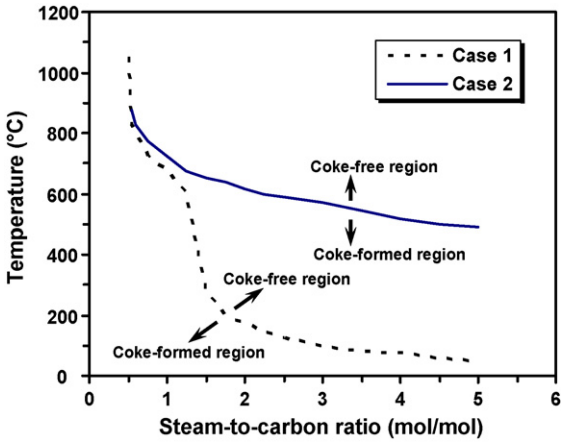

Fig. 3. Coke formation boundary of DME SR as a function of steam-to-carbon (S/C) and temperature.

conversion of DME could be achieved when the temperature and S/C are higher than 200 °C and 1.5 (the stoichiometric ratio of DME SR), respectively. Increase in S/C and in temperature enhanced the conversion until it reached 100%. However, the complete conversion could not be achieved when S/C was below 0.5. DME could not be reformed in the absence of steam in this case. According to the experimental data, DME could be completely converted when the reforming temperature was above 350 °C [9–11].

3.3. Hydrogen yield

Fig. 5 shows the hydrogen yield of DME SR as a function of S/C and temperature. Theoretically, 1 mole of DME gives 6 mole of hydrogen by steam reforming of DME.

In Fig. 5a (Case 1), H_2 yield was promoted by increasing temperature. When S/C is higher than 1.5, the maximum yield of 90% was found at T_r range of ca. 600–700 °C. Further increase in T_r brought about the decrease in the yield due to the r-WGSR. H_2 was not produced at the temperature lower than ca. 200 °C. In Fig. 5b (Case 2), H_2 yield was obtained at 33.3% when the temperature was below ca. 400 °C. This result is consistent with DME conversion and coke formation contributed by reaction (18). H_2 yield increased when S/C and temperature increased up to 5 and ca. 500 °C, respectively. The maximum yield of 95% was achieved at S/C = 5 and T_r = 500 °C.

As for Case 3 in Fig. 5c, increasing S/C improved the H_2 yield since DME conversion was expedited and r-WGSR was inhibited. The H_2 yield of above 99% was achieved at S/C > 2 and T_r = 125–250 °C. Upon a complete conversion of DME at a given S/C ratio, the H_2 yield decreased monotonously as the reforming temperature increased. The thermodynamic result shows similar tendency with the experimental one although the experiment proceeds below the equilibrium [9,11]. High space time may be needed for approaching the equilibrium of DME SR. As shown in Fig. 5d (Case 4), the H_2 yield was lower than that obtained from Case 1 at low S/C ratios because methane was formed instead of hydrogen and coke. When the reforming condition fell into the coke-free region of

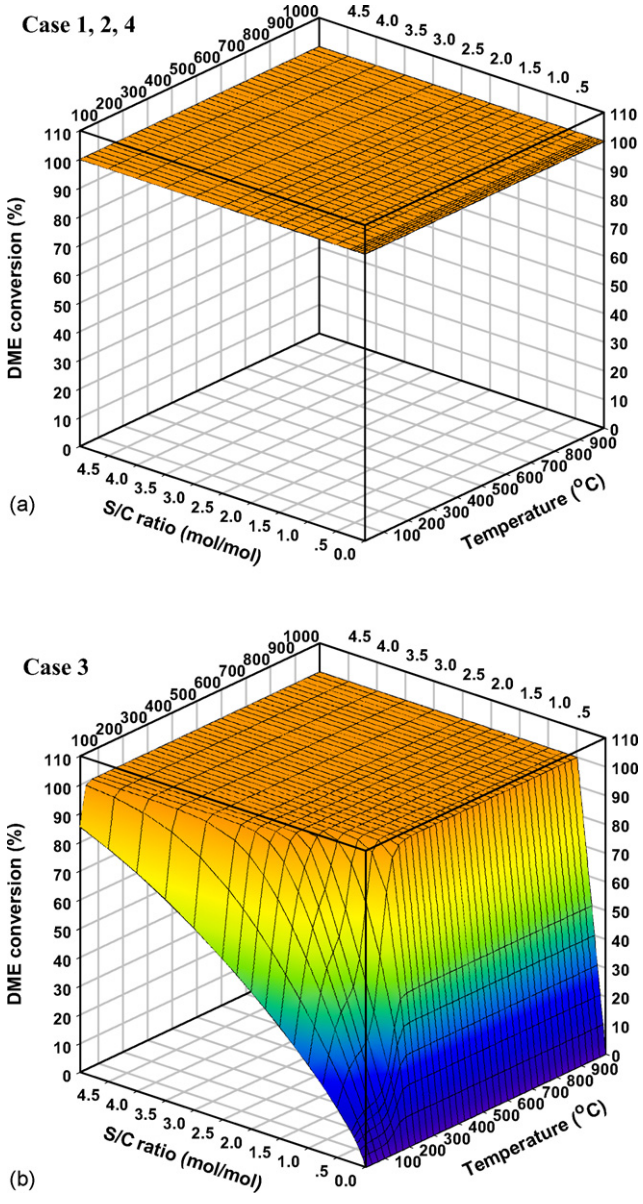

Fig. 4. Equilibrium conversion of DME as a function of steam-to-carbon (S/C) and temperature: (a) Cases 1, 2 and 4 and (b) Case 3.

Case 2, the H_2 yield from Cases 1, 2, and 4 becomes comparable. Even at S/C = 0, hydrogen yield could be achieved up to 50% yield for Cases 1 and 2, and to ca. 18% for Case 4. Hydrogen could not however be produced when the temperature were below 200 and 400 °C for Cases 1 and 4, respectively. Coke formation should be seriously considered under the dry condition.

High S/C and T_r enhanced the reforming performance in terms of carbon inhibition, DME conversion and hydrogen yield. However, the higher S/C requested higher reactor volume because of higher steam volumetric flow, and consumed higher input heat duty because of higher vaporization energy. Therefore, optimization of overall efficiency of fuel cell system is required for selection of suitable operating condition of the reformer.

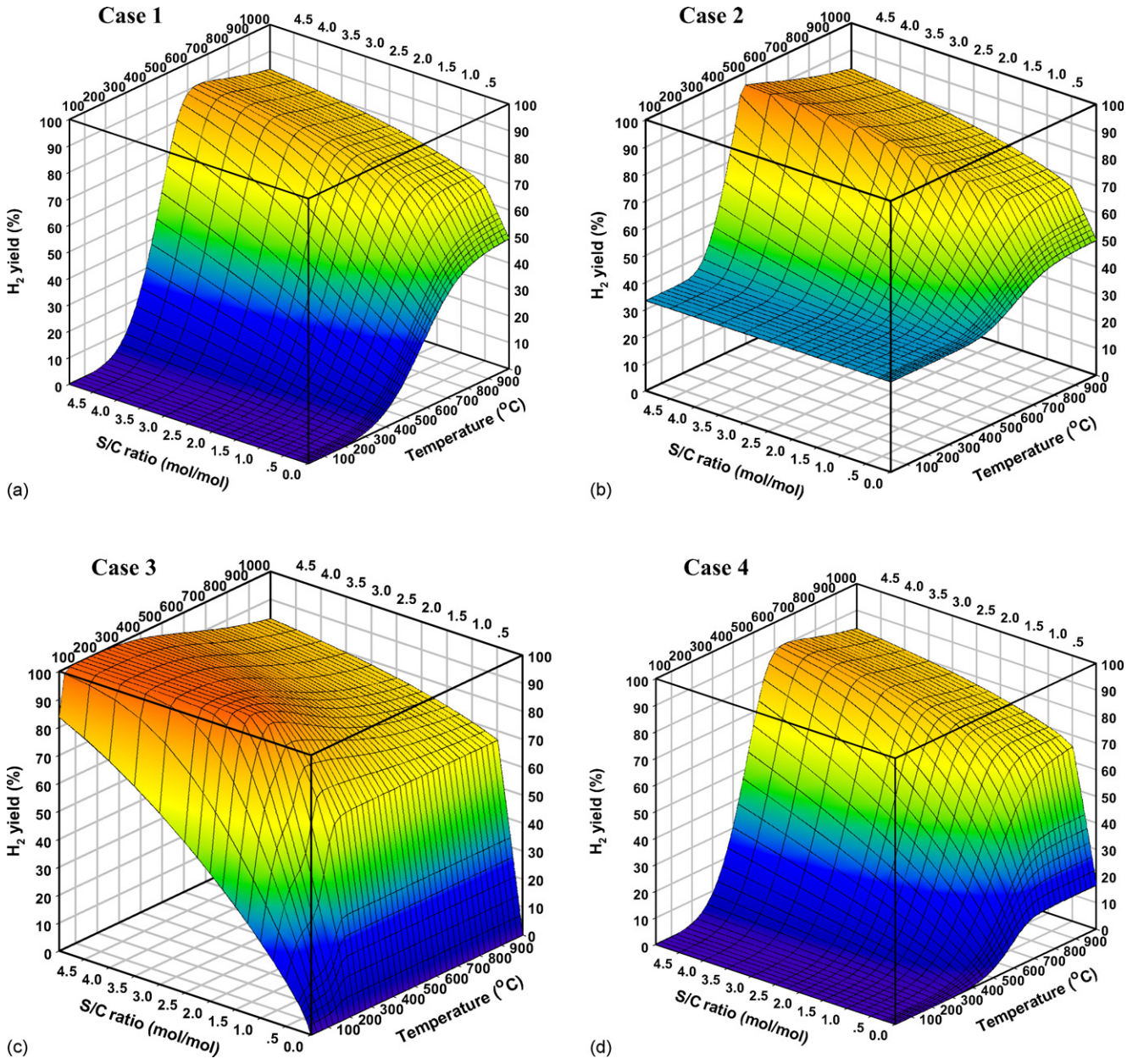

Fig. 5. Equilibrium hydrogen yield as a function of steam-to-carbon (S/C) and temperature: (a) Case 1; (b) Case 2; (c) Case 3; (d) Case 4.

4. Conclusions

Thermodynamic equilibrium of dimethyl ether steam reforming (DME SR) was studied by Gibbs free minimization for carbon formation boundary, DME conversion and hydrogen yield in an external reformer. Effect of steam-to-carbon ratio (S/C = 0–5) and reforming temperature (25–1000 °C) and product basis species were investigated. The results indicated that carbon formation could be avoided by increasing the steam-to-DME ratio and/or by increasing the reforming temperature.

Based on the compound basis set DME, methanol, CO_2, CO, H_2, H_2O and coke, complete conversion of DME and hydrogen yield above 78% were achieved in the coke-free region at the normal operating temperature of 600 °C for MCFC and that of 900 °C for SOFC. When methane was taken into account, coke formation was significantly suppressed. Hydrogen yield up to almost 100% could be achieved at S/C > 2 and T_r = 125–250 °C when coke and methane were thermodynamically unfavorable. It should be realized that in the experiment carbon may not be formed as graphite and consequently the calculation data may deviate from the experiment. Reaction mechanisms, i.e. kinetic control or heat and mass transfer control, would also affect the result of DME SR in practical applications.

References

[1] F.S. Ramos, A.M. Duarte de Farias, L.E.P. Borges, J.L. Monteiro, M.A. Fraga, E.F. Sousa-Aguiar, L.G. Appel, Catal. Today 101 (2005) 39–44.
[2] D. Mao, W. Yang, J. Xia, B. Zhang, G. Lu, J. Mol. Catal. A 250 (2006) 138–144.

[3] J. Fei, X. Tang, Z. Huo, H. Lou, X. Zheng, Catal. Commun. 7 (2006) 827–831.
[4] J. Fei, Z. Hou, B. Zhu, H. Lou, X. Zheng, Appl. Catal. A: Gen. 304 (2006) 49–54.
[5] Chemical Week, 168(2) (2006) 16.
[6] V.V. Galvita, G.L. Semin, V.D. Belyaev, T.M. Yurieva, V.A. Sobyanin, Appl. Catal. A: Gen. 216 (2001) 85–90.
[7] K. Takeishi, H. Suzuki, Appl. Catal. A: Gen. 260 (2004) 111–117.
[8] T. Matsumoto, T. Nishiguchi, H. Kanai, K. Utani, Y. Matsumura, S. Imamura, Appl. Catal. A: Gen. 276 (2004) 267–273.
[9] Y. Tanaka, R. Kikuchi, T. Takeguchi, K. Eguchi, Appl. Catal. B: Environ. 57 (2005) 211–222.
[10] T. Mathew, Y. Yamada, A. Ueda, H. Shioyama, T. Kobayashi, Appl. Catal. A: Gen. 286 (2005) 11–22.
[11] K. Faungnawakij, Y. Tanaka, N. Shimoda, T. Fukunaga, S. Kawashima, R. Kikuchi, K. Eguchi, Appl. Catal. A: Gen. 304 (2006) 40–48.
[12] T.A. Semelsberger, K.C. Ott, R.L. Borup, H.L. Greene, Appl. Catal. A: Gen. 309 (2006) 210–223.
[13] K. Faungnawakij, R. Kikuchi, K. Eguchi, J. Power Sources 161 (2006) 87–94.
[14] W. Sangtongkitcharoen, S. Assabumrungrat, V. Pavarajarn, N. Laosiripojana, P. Praserthdam, J. Power Sources 142 (2005) 75–80.
[15] V. Mas, R. Kipreos, N. Amadeo, M. Laborde, Int. J. Hydrogen Energy 31 (2006) 21–28.
[16] T.A. Semelsberger, R.L. Borup, J. Power Sources 152 (2005) 87–96.
[17] R.H. Perry, D.W. Green, J.O. Maloney, Perry's Chemical Engineers' Handbook, McGraw-Hill, New York, 1999.
[18] J.N. Armor, Appl. Catal. A: Gen. 176 (1999) 159–176.